11th International Symposium on Turbulence and Shear Flow Phenomena (TSFP11)
Southampton, UK, July 30 to August 2, 2019

EFFECT OF THE INTERMITTENCY ON THE OUTER SCALES IN TURBULENT BOUNDARY LAYERS

Nico Reuther and Christian J. Kähler
Institute for Fluid Mechanics and Aerodynamics
Universität der Bundeswehr München
Werner-Heisenberg-Weg 39, 85577 Neubiberg, Germany
Nico.Reuther@unibw.de

ABSTRACT

The intermittency between laminar and turbulent flow regions has been a topic of interest for decades. Detecting the complex interface between irrotational laminar and rotational turbulent fluid and understanding the physical processes occurring at the interface have achieved large progress thanks to advances in spatio-temporal resolved numerical and experimental techniques. However, with respect to turbulence statistics, the intermittent feature has been almost completely neglected and statistical averaged quantities were obtained by averaging over rotational and irrotational flow regions. Exclusively, Jiménez *et al.* (2010) studied mean quantities conditioned to the turbulent/non-turbulent interface (TNTI). Based on this, they found the rotational flow state to feature a tangential Reynolds stress $\langle uw \rangle > 0$ in the outer region of the boundary layer. This contradicts the common assumption that this quantity is negative everywhere in the flow. On the basis of these results, this work examines the effect of the two distinct flow states on the statistics of a high Reynolds number turbulent boundary layer measured with PIV. In particular, the impact of intermittency on fluctuating velocities and higher order statistics is discussed.

INTRODUCTION

The intermittent nature of a free shear flow was first revealed in the 1940s. Using hot-wire anemometry, Corrsin (1943) visualized the bimodal properties of the flow by plotting the temporal evolution of streamwise velocity at a fixed wall-normal location. While the signal showed strong turbulent fluctuations for some time periods, an almost constant velocity was observed for others. Based on these findings, further studies were conducted with respect to wall-bounded flows and similar temporal state changes were found (Corrsin & Kistler, 1955; Klebanoff, 1955). This resulted in the first schematic image of a turbulent boundary layer with its highly complex folded interface as we know it today.

With the aim to reveal further details of the motions inside a turbulent boundary layer, Kovasznay *et al.* (1970) performed zonal sampling and averaging. By analyzing hot-wire signals and choosing an appropriate threshold that associates smaller fluctuations with noise, they classified the flow as turbulent or non-turbulent, respectively. Based on this classification, zonal averages were calculated, which were subsequently used to decompose the total velocity. This promising technique was later applied in further studies (Antonia, 1972; Hedley & Keffer, 1974), but its application so far remained limited to single-point measurements.

In order to study the effect of intermittency on turbulent statistics, Jiménez *et al.* (2010) analyzed conditional statistics using DNS of a turbulent boundary layer at $Re_\theta = 1550$. Using a vorticity magnitude criteria, they divided the flow into turbulent and non-turbulent regions and calculated the mean streamwise velocity and the Reynolds stresses for each flow state separately. By this means, a positive tangential Reynolds stress was found in the outer turbulent region of the boundary layer.

Kwon *et al.* (2016) proposed an interface height based decomposition to evaluate the effect of the intermittency on the outer scales in a turbulent boundary layer. A comparison of fluctuation fields in conjunction with the instantaneous TNTI revealed that the traditional Reynolds decomposition causes strong positive fluctuations in the potential flow regime. On the other hand, fluctuating velocities close to zero were found in the laminar region under the interface height based decomposition. In addition, a comparison of statistically averaged quantities showed that the outer scales are significantly biased as a result.

Since the decomposition technique by Kwon *et al.* (2016) is only applicable in flows where the variation in Reynolds number in streamwise direction is negligibly small, this study analyzes the application of the zonal decomposition by Kovasznay *et al.* (1970) to make a statistical analysis of the intermittent properties possible. Therefore, large-scale PIV measurements were performed to resolve the evolution of a zero-pressure gradient turbulent boundary layer at a high Reynolds number over multiple boundary layer thicknesses in streamwise direction.

MEASUREMENT

Measurements were conducted in the atmospheric wind tunnel at the Bundeswehr University in Munich (AWM). The Eiffel type tunnel has a 22 m-long test section and a 1.85 m $\times$ 1.85 m cross section. Freestream velocities of up to 40 m/s can be obtained in the facility. The boundary layer of interest develops along the side wall of the test section, where a model is installed with the intent to investigate turbulent boundary layers subjected to strong adverse pressure gradients (Novara *et al.*, 2016; Reuther & Kähler, 2018). For simplification reasons, this work solely focuses on the flat plate region. Statistic pressure measurements

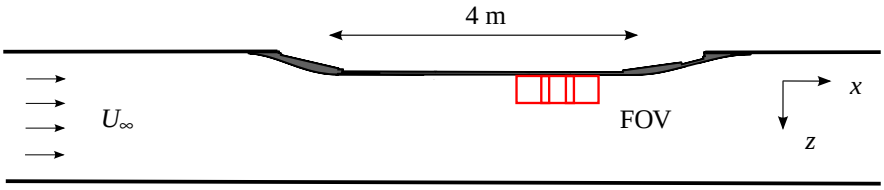

Figure 1: Schematic of the boundary layer model and the experimental setup (top view). Red rectangles indicate single fields of view (FOVs).

conducted over the model reveal a vanishing pressure gradient at the location of the field of view (FOV). The statistics compare well with other facilities at similar Reynolds numbers. Figure 1 shows a schematic of the boundary layer experiment and the experimental setup. Here, the coordinate systems x, y, and z refer to the streamwise, spanwise, and wall-normal directions with U, V, and W describing the related velocity components.

Large-scale two-component PIV was performed to resolve the full boundary layer in the zero-pressure gradient region at a friction Reynolds number of $Re_\tau \approx 9{,}300$. This corresponds to an inflow velocity of 23 m/s. Due to the contraction the freestream velocity at the model is approximately 28 m/s. To observe the particle displacement three sCMOS cameras (image sensor size: 2560 $\times$ 2160 px) equipped with 50 mm Zeiss lenses were installed on top of the tunnel, resulting in an FOV of 0.8 m $\times$ 0.24 m. Illumination of the tracer particles was realized by means of a Spectra Physics Quanta-Ray PIV 400 laser. The polished flat aluminum plate was illuminated tangentially to avoid undesirable diffuse reflections at the wall (Kähler *et al.*, 2006).

To obtain converged statistical averaged quantities, 15,000 double-frame images were recorded. Single large-scale PIV recordings were evaluated using iterative multi-pass window-correlation approaches with image deformation (Raffel *et al.*, 2018). Here, final interrogation window sizes of 16 $\times$ 16 px were applied with an overlap of 50 %.

TNTI DETECTION

In order to segment the irrotational from the rotational fluid and to apply the decomposition by Kovasznay *et al.* (1970), the instantaneous interface needs to be detected first. Identifying the highly curved TNTI experimentally or numerically is challenging. Turbulence is characterized by its unsteadiness in space and time and by its vorticity and diffusivity. Therefore, vorticity based criteria were the preferred method for interface detection in the past. However, if the spatial resolution is restricted by experimental limitations (e.g. camera sensor size), the vorticity magnitude is not sufficiently resolved, which in turn prevents an accurate detection of the TNTI. Therefore, Chauhan *et al.* (2014) introduced a method based on the magnitude of the turbulent kinetic energy in the frame of reference moving with the local freestream velocity. Thus, regions featuring a streamwise velocity close to the U_∞ were considered as non-turbulent. Besides the fact that estimating the turbulent kinetic energy is not that simple, this technique prevents the detection of turbulent bulges exhibiting a streamwise velocity of close to U_∞. Furthermore, laminar flow regions whose velocity does not match U_∞ are considered as turbulent flow regions although they do not exhibit the characteristic turbulent properties mentioned before.

To overcome those drawbacks, Reuther & Kähler (2018) have developed TNTI detection criteria that are applicable to velocity fields featuring a lower spatial resolution and higher uncertainty as known from DNS. A passive scalar method based on the particle image density was found to be the most accurate and robust method to resolve small scales. In addition, the approach is not biased by potential flow fluctuations as it solely resolves the turbulent flow field. For this reason, however, it is not suitable for a joint turbulent and potential flow analysis as intended in this study. Therefore, the homogeneity criterion introduced in Reuther & Kähler (2018) is best suited to distinguish between turbulent and non-turbulent flow regions. In contrast to prior TNTI detection approaches, this method resolves the main characteristic of the non-turbulent flow. Deviations from the real interface are relatively small and have only a negligible effect on the statistical evaluation, although bias errors occur due to spatial averaging.

VELOCITY PROFILES

Based on the subdivision of instantaneous velocity fields into turbulent and non-turbulent flow regions by means of applying the homogeneity criterion, conditioned statistics with respect to each kind of the flow state were obtained. Figure 2 presents mean velocity profiles for the intermittent region of the boundary layer. From the results, it is evident that the velocity increase in the outer region with respect to the log-layer region coincides with the intermittent region. This is due to the fact that the laminar flow regions maintain their momentum to a large extend as visi-

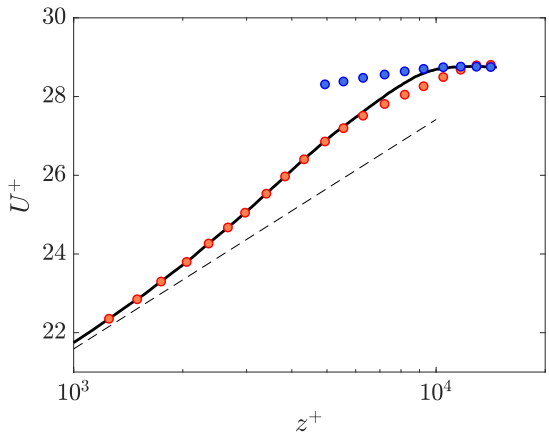

Figure 2: Velocity profiles conditioned to the TNTI scaled in inner units. —— Unconditioned average; ● turbulent mean; ● non-turbulent mean. The dashed line is $\log(z^+)/0.395 + 4.1$.

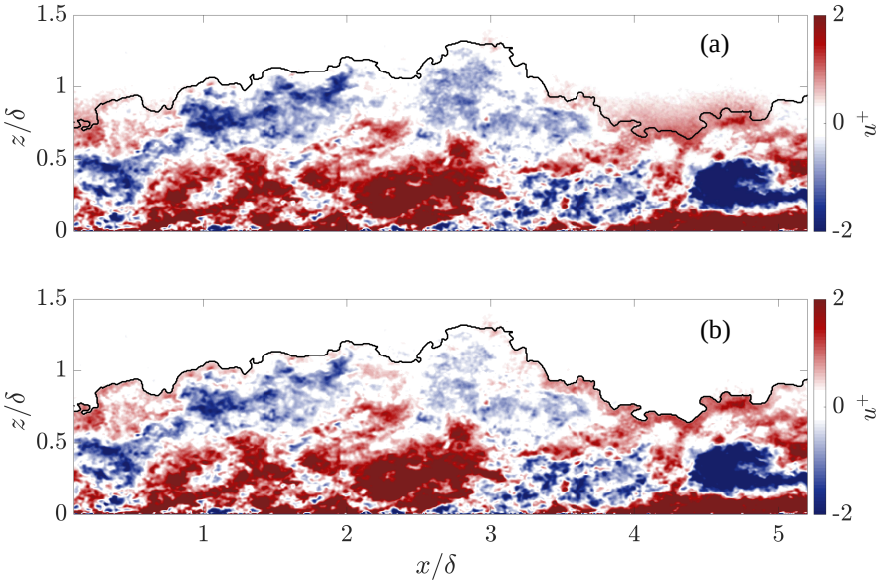

Figure 3: Streamwise velocity fluctuations obtained when applying (a) the traditional Reynolds decomposition and (b) the zonal decomposition. Black line indicates TNTI.

ble in the figure (blue circles). However, also the mean velocity profile determined only on the turbulent parts of the boundary layer lead to a strong deviation to the log-layer slope. This implies that the laminar flow regions, entering the turbulent boundary layer due to intermittency, transfer their momentum into the turbulent regions. In effect the turbulent bulges are accelerated due to the action of entrainment of laminar high momentum fluid. Due to the momentum transfer, potential flow regions are decelerated with increasing wall proximity. This explains the slight slope of the blue symbols in figure 2. This physical mechanism in the outer region does not exist in the inner layer and this causes a different scaling of the two regions, which is well known as inner and outer scaling.

These observations agree well with DNS data at $Re_\theta \approx 1550$ presented by Jiménez *et al.* (2010), which indicates that the applied TNTI detection approach allows for an adequate conditioned statistical analysis. However, it should be noted that the uncertainty in the innermost intermittent region for the non-turbulent average and in the outermost intermittent region for the turbulent mean, respectively, increases due to the decreasing frequency of occurrence and the limited number of recorded images.

TURBULENCE INTENSITIES

While the uncertainty of velocity estimations is solely linked to the measurement and PIV evaluation uncertainties, the uncertainty of turbulence intensity determination is additionally dependent on the way of decomposing the total velocity into a mean and a fluctuating component and the convergence of the mean quantities. The traditional Reynolds decomposition approach is widely accepted for higher order statistics. However, Kwon *et al.* (2016) demonstrated the deficiencies of this approach and proposed a novel decomposition method based on the instantaneous interface height as outlined before. Using this method, the interface fluctuations are not considered as turbulence. Consequently, turbulent fluctuations are not biased by the unsteadiness of the laminar potential flow. However, a drawback of this approach is its limitation to a rather constant Reynolds number flows. In other words, it is barely applicable to pressure gradient or non-stationary flows for instance. Therefore, this work extends the Kovasznay *et al.* (1970) zonal decomposition concept to 2-dimensional data. Thus, the local total velocity was decomposed as follows

$$\begin{aligned} U_\mathrm{t}(x,z) &= \bar{U}_\mathrm{t}(x,z) + u_\mathrm{t}(x,z) \\ U_\mathrm{nt}(x,z) &= \bar{U}_\mathrm{nt}(x,z) + u_\mathrm{nt}(x,z) \end{aligned} \tag{1}$$

Here, the indices ‘t’ and ‘nt’ refer to the kind of flow (‘t’ - turbulent; ‘nt’ - non-turbulent). To illustrate the effect of the decomposition techniques, velocity fluctuation fields are shown in figure 3 for both the traditional Reynolds decomposition and the zonal decomposition. Here, the major deficiency of the traditional Reynolds decomposition is obvious. The potential flow regions are wrongly considered as turbulent flow regions although they are laminar in nature. In effect the turbulent fluctuations appear amplified in the statistical representation, see figure 4. Furthermore, the laminar fluctuations contribute in a PDF to the positive fluctuations while the negative fluctuations are associated with the real turbulent fluctuations as shown exemplary for $z/\delta = 0.9$ in figure 5.

Similar to the interface height based decomposition by Kwon *et al.* (2016), interface fluctuations are not considered as turbulence in case of the zonal decomposition as evident in figure 3. Moreover, the turbulent fluctuating velocities change according to the change in mean velocity illustrated in figure 2. Due to the lower turbulent mean value, this results in a shift to more positive values.

Based on the traditional Reynolds decomposition and the zonal decomposition, turbulence intensities were calculated. Figure 4 presents the unconditional and conditioned mean quantities scaled in outer units for a better representation of the methods deviations. From the results, it is evident that the irrotational fluid carries a large amount of ‘turbulent’ kinetic energy if the intermittent behavior is not

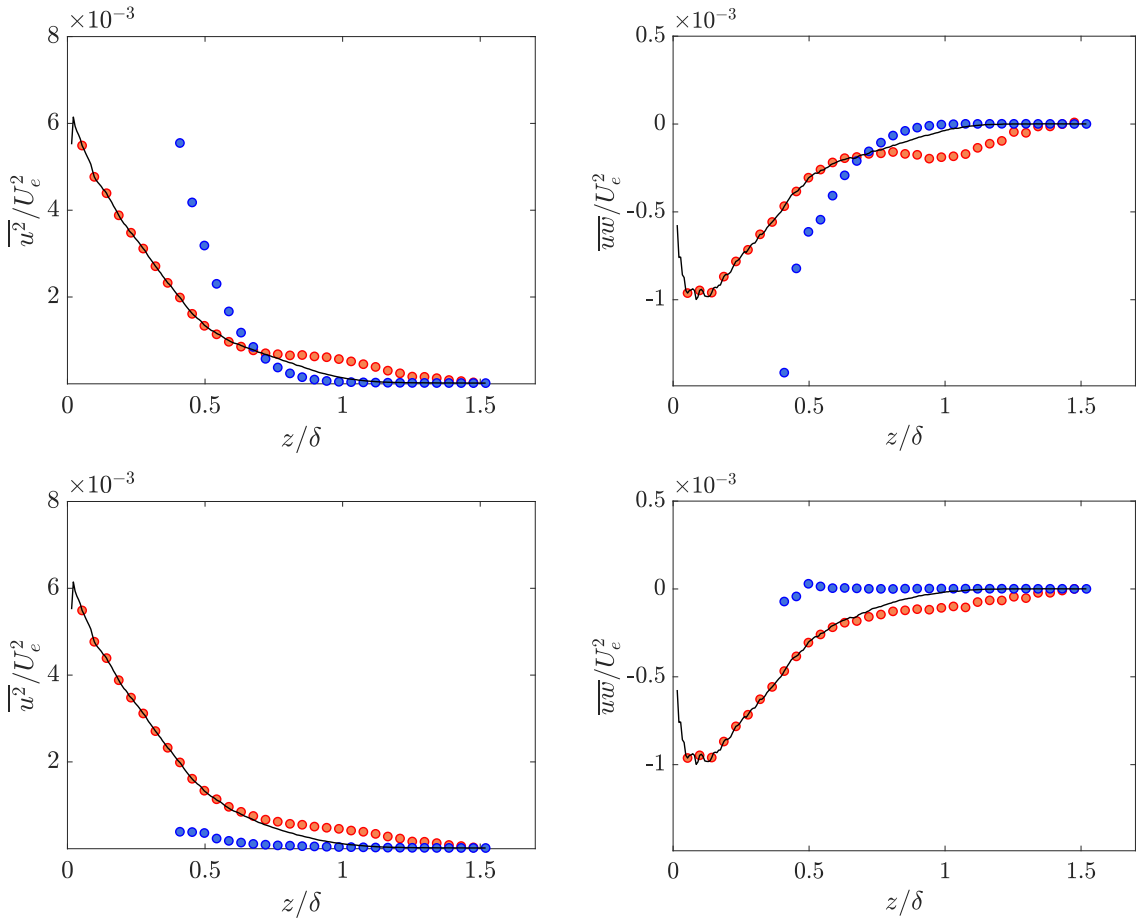

Figure 4: Normal and shear stress intensities under the traditional Reynolds decomposition (top) and the zonal decomposition (bottom). —— Unconditioned average; ● only turbulent; ● only non-turbulent.

accounted for during decomposition. This contradicts the general understanding of the potential flow. On the contrary, when considering the unsteadiness by applying the zonal decomposition, this non-turbulent large-scale energy is removed. In addition, a decrease in turbulent streamwise turbulence intensity is observed in the region where the intermittent feature is strong ($0.7 < z/\delta < 1.2$). With respect to unconditional results, figure 4 indicates that the distribution is also losing its little bump in this region. This holds for the streamwise but also for the shear turbulence intensities. Finally, the shear turbulence intensity distribution under the zonal decomposition reveals that the production of turbulent energy $-\langle uw \rangle \, \partial U/\partial z$ is equal to zero almost everywhere in the potential flow while it is positive everywhere in the turbulent flow region. Which contradicts observations by Jiménez *et al.* (2010).

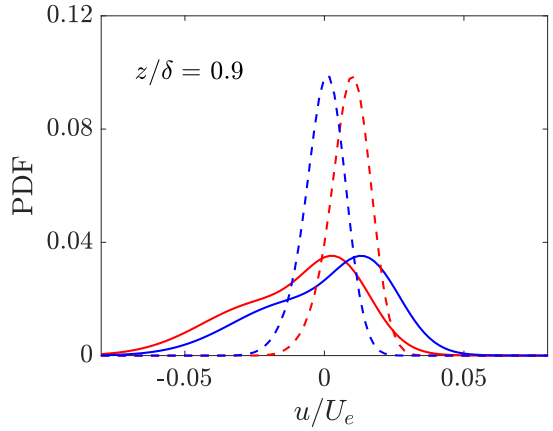

Figure 5: Probability density function of turbulent (solid lines) and non-turbulent (dashed lines) fluctuating velocities under the traditional Reynolds decomposition (red) and zonal decomposition (blue).

SUPERSTRUCTURES

Based on these findings, the effect of the averaging concept on the size and shape of turbulent superstructure will be outlined next using a two-point correlation approach. As discussed above, the traditional Reynolds decomposition leads to artificial turbulent fluctuations in the potential flow field, which are exclusively due to the TNTI fluctuations. Consequently, the classical two-point correlation approach will include these virtual 'turbulent' fluctuations. As a result, the two-point correlation map of streamwise velocity fluctuations is biased in the outer intermittent region. By means of applying their new decomposition approach, Kwon *et al.* (2016) found that the large-scale coherence extent is significantly smaller in the outer region than previously thought (Hutchins & Marusic, 2007; Lee & Sung, 2011). However, two crucial points were neglected. First, with increasing wall distance the probability that the correlation point is instantaneously

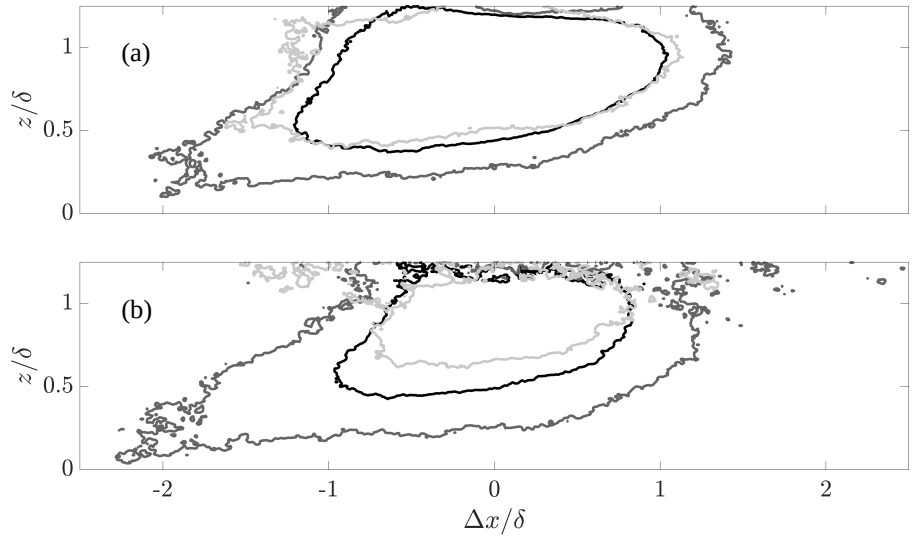

Figure 6: Two-point correlation map of streamwise velocity fluctuations using the (*a*) classical and (*b*) modified approach at a reference wall-normal position of $z/\delta = 0.8$. Contours are plotted for 0.15. Black line indicates unconditional results while the gray lines present conditional results: light gray line ($u > \sigma$), dark gray line ($u < \sigma$).

located in the potential flow region rises. In that case, a strong coherence with the potential flow neighboring vectors is observed as the potential flow fluctuations are quite homogeneous in magnitude and direction in contrast to real turbulent fluctuations. Second, the correlation point is generally correlated with the full FOV, although by definition superstructures are only found in the turbulent regime.

Therefore, this work applies a modified two-point correlation approach where the correlation point is solely correlated with the rotational fluid regions. Furthermore, it verifies that the point of interest is located in the turbulent regime. Otherwise the velocity field is excluded for correlation purposes. Figure 6 shows results of the classical and the modified two-point correlation approach. While fluctuating velocities are obtained using the traditional Reynolds decomposition in case of the classical approach, the zonal decomposition is applied in case of the modified one. As a result of the revisions, the superstructure extent decreases substantially for correlation points in the outer region. This is in good agreement with the results by Kwon *et al.* (2016). Note, due to the smaller number of samples associated with the specific selection process, the correlation function shows a noisy nature in the outermost region.

Finally, two-point correlations were conditioned to the sign and magnitudes of streamwise velocity fluctuations in order to exclusively consider strong events (Buchmann *et al.*, 2014). In other words, if the fluctuating velocity at a time step t exceeds the local standard deviation σ at the reference position, the fluctuation field is considered. If not, the time step is excluded from two-point correlation. By this means, it is found that structures featuring strong positive streamwise fluctuating velocities exhibit only half the size of those featuring strong negative streamwise fluctuating velocities.

CONCLUSIONS

The analysis illustrates the strong effect of the averaging procedure applied in the intermittent flow region on the statistical and structural features of turbulent boundary layers. As a result, following crucial points should be considered when analyzing turbulent flows where the intermittency plays a dominant rule:

- Due to the unsteadiness of the TNTI, the traditional Reynolds decomposition causes strong fluctuations in the potential flow region. Hence, it is not recommended to apply this technique in the intermittent region.
- If the interface height based decomposition by Kwon *et al.* (2016) is not applicable, the zonal decomposition concept by Kovasznay *et al.* (1970) allows an adequate representation of the potential flow fluctuations.
- A conditional statistical analysis, which considers the two distinct flow states separately, allows to analyze the performance of the decomposition technique applied. Moreover, it contributes to the understanding of the dynamics of turbulent flows.
- For an accurate large-scale coherence analysis using two-point correlations, a decomposition method is of great importance, which ensures that the potential flow region does not exhibit any fluctuations due to the TNTI variations. In addition, a method that exclusively correlates the reference point with the turbulent regime, where the superstructures are found by definition, is recommended for proper length scale analysis.

REFERENCES

Antonia, R. A. 1972 Conditionally sampled measurement near the outer edge of aturbulent boundary layer. *J. Fluid Mech.* **56**, 1–18.

Buchmann, N. A., Kücükosman, Y. C., Ehrenfried, K. & Kähler, C. J. 2014 Wall pressure signature in compressible turbulent boundary layers. In *Progress in Wall Turbulence: Understanding and Modelling*.

Chauhan, K., Philip, J., de Silva, C. M., Hutchins, N. & Marusic, I. 2014 The turbulent/non-turbulent interface and entrainment in a boundary layer. *J. Fluid Mech.* **742**, 119–151.

Corrsin, S. 1943 Investigation of flow in an axially symmetrical heated jet of air. *Tech. Rep.*. NACA WR W-94.

Corrsin, S. & Kistler, A. L. 1955 Free-Stream Boundaries of Turbulent Flows. *Tech. Rep.*. NACA-TR-1244.

Hedley, T. B. & Keffer, J. F. 1974 Some turbulent/non-turbulent properties of the outer intermittent region of a boundary layer. *J. Fluid Mech.* **64**, 645–678.

Hutchins, N. & Marusic, I. 2007 Evidence of very long meandering features in the logarithmic region of turbulent boundary layers. *J. Fluid Mech.* **579**, 1–28.

Jiménez, J., Hoyas, S., Simens, M. P. & Mizuno, Y. 2010 Turbulent boundary layer and channels at moderate Reynolds numbers. *J Fluid Mech.* **657**, 335–360.

Kähler, C. J., Scholz, U. & Ortmanns, J. 2006 Wall-shear-stress and near-wall turbulence measurements up to single pixel resolution by means of long-distance micro-PIV. *Exp. Fluids* **41**, 327–341.

Klebanoff, P. S. 1955 Characteristics of turbulence in a boundary layer with zero pressure gradient. 1135-1153. NACA-TR-1247.

Kovasznay, L. S. G., Kibens, V. & Blackwelder, R. F. 1970 Large-scale motion in the intermittent region of a turbulent boundary layer. *J. Fluid Mech.* **41**, 283–325.

Kwon, Y. S., Hutchins, N. & Monty, J. P. 2016 On the use of the Reynolds decomposition in the intermittent region of turbulent boundary layers. *J. Fluid Mech.* **794**, 5–16.

Lee, J. H. & Sung, H. J. 2011 Very-large-scale motions in a turbulent boundary layer. *J. Fluid Mech.* **673**, 80–120.

Novara, M., Schanz, D., Reuther, N., Kähler, C. J. & Schröder, A. 2016 Lagrangian 3D particle tracking in high-speed flows: Shake-The-Box for multi-pulse systems. *Exp. Fluids* **57**, 128.

Raffel, M., Willert, C. E., Scarano, F., Kähler, C. J., Werely, S. T. & Kompenhans, J. 2018 *Particle Image Velocimetry - A Practical Guide*. Springer International Publishing.

Reuther, N. & Kähler, C. J. 2018 Evaluation of large-scale turbulent/non-turbulent interface detection methods for wall-bounded flows. *Exp. Fluids* **59**, 121.